Molecular Association in Ethanol-Water Mixtures Studied by Mass Spectrometric Analysis of Clusters Generated through Adiabatic Expansion of Liquid Jets

Nobuyuki Nishi,* Kunimasa Koga,*,† Chikako Ohshima,† Kazunori Yamamoto, Umpei Nagashima, and Kenzo Nagami*,†

Contribution from the Institute for Molecular Science, Myodaiji-cho, Okazaki 444, Japan, and Suntory Research Center, Wakayamadai 1-1-1, Shimamoto-cho, Mishima-gun, Osaka 618, Japan. *Received December 21, 1987*

Abstract: Molecular association in ethanol-water solutions with various ethanol concentrations was studied mass spectrometrically by isolating the clusters through adiabatic expansion of liquid jets under vacuum. The spectral pattern of the clusters changed sensitively depending on the ethanol concentration region. In the region of x (ethanol mole fraction) < 0.04, ethanol monomer and polymer signals are followed by long water sequences of hydrated species $(C_2H_5OH)_m(H_2O)_n$. At low temperatures, ethanol-ethanol hydrogen bond formation becomes predominant and water molecules tend to participate in hydrophobic hydration of the ethyl groups of the polymer chains. This water shell was not seen for the mixtures with $x > 0.04$. At $x = 0.08$, the growth of ethanol polymers is almost saturated, and in the region of $0.08 \leq x \leq 0.5$ the spectral pattern showed little change although the polymer intensity was strongest for the solution with $x = 0.42$ at 35 °C. In ethanol-rich solutions, the intensity of the polymers becomes weaker with decreasing water content. Neat ethanol did not produce large polymers any more. The observed changes of the cluster spectra coincided nicely with the reported NMR data and thermodynamic properties of this system, providing the molecular level information on the microstructures. The present study makes the nature of ethanol-water mixtures clearly understandable at a molecular level: (1) the hydrophobic hydration of ethanol is so strong that pure water clusters are not detectable at $x > 0.04$ and (2) ethanol molecules tend to form ethanol polymers with surrounding water molecules. Ab initio calculations of the bond energies of the gas-phase dimers formed from ethanol and water were also carried out by using the 6-31G** basis set and showed that the ethanol-ethanol hydrogen-bond energy (5.66 kcal/mol) is nearly the same as those of the water-water and the water-ethanol bond energies (5.4-5.85 kcal/mol). This result supported the experimental conclusion that the trend in ethanol polymer formation is due to an environmental effect induced by the presence of water molecules surrounding ethanol molecules.

I. Introduction

A new molecular beam technique isolating clusters from liquid solutions was developed by the method of adiabatic expansion of mist particles under vacuum.[1] In the previous report, the observed cluster distribution was analyzed in terms of the equilibrium constants of the molecular exchange processes between clusters and free molecules in liquid. A constant κ_m for a hydrated cluster $X_m(H_2O)_n$ was introduced to describe the stability of the hydrated cluster and it corresponds to an nth part of the equilibrium constant for the following exchange process: $X_{m-1}(H_2O)_n + X \rightleftarrows X_m(H_2O)_{n-1} + H_2O$. For ethanol and 2-propanol, the equilibrium was found to be largely shifted to the right side. Even at an ethanol mole fraction of 0.01, ethanol molecules tend to associate at lower temperatures and the enthalpy change of the above exchange process was in the range of 4.5 ± 0.6 kcal/mol for $1 \leq m \leq 3$. This stability was attributed to the hydrophobic hydration of water molecules to the ethyl groups.

Ethanol-water mixtures are frequently used as solvents in studies of chemical equilibria and reactions as well as various biological studies. As stated by Franks and Ives, the relatively simple alcohol-water mixtures may serve as models helpful for a better understanding of more complex systems.[2] This system shows abnormalities in properties such as negative partial molar volumes,[3,4] differential heats of solution,[5] and the chemical shift of water hydrogen.[6,7] Coccia et al. presented evidence that addition of small quantities of ethanol to water promotes hydrogen bonding association among water molecules at ethanol molar fractions (x) lower than 0.08, and at $0.25 \leq x \leq 0.75$ the water structures are progressively disrupted by increasing alcohol concentration.[7] At $x = 0.08$ the partial molar volume of ethanol becomes minimum and that of water attains its maximum value.[3] Franks and Ives said that the oddities in observed properties are structural in origin, and will eventually be understood in the light of full knowledge of the "structural behavior" of the components.[3] Here we report new information on association in ethanol-water mixtures in terms of molecular composition of stable clusters that provides reasonable elucidation of the oddish properties on a molecular level. From a theoretical point of view, Ben-Naim presented a new procedure which provides information on the affinity between two species in a mixture of two components.[8] Application of this procedure to the ethanol-water system produced very interesting behavior for the quantity G_{AW} which is defined as an integral over the pair correlation function between ethyl alcohol and water molecules. This quantity conveys the average affinity of alcohol to water molecules. The derived G_{AW} showed a very steep decrease with increasing alcohol in water media and its minimum appeared at $x \approx 0.4$ indicating that ethanol-water interactions become weakest at this concentration. On the other hand, he also found that the quantity G_{AA} (average affinity between alcohol molecules) attains a maximum at $x \approx 0.1$. This was attributed to an enhancement in the strength of hydrophobic interactions. Apart from the explanation on the reason, the appearance of the critical concentrations has also been observed in the present mass spectrometric analysis of the clusters.

The method used here is essentially the mass spectrometry of smallest fractions of liquid. Although the energy of the ionizing electrons is not so large (40 eV), the analyzer makes the clusters

*Address correspondence to this author at the Institute for Molecular Science.
†Suntory Research Center.

(1) Nishi, N.; Yamamoto, K. *J. Am. Chem. Soc.* **1987**, *109*, 7353.
(2) Franks, F.; Ives, D. J. G. *Q. Rev. Chem. Soc.* **1966**, *20*, 1.
(3) Mitchell, A. G.; Wynne-Jones, W. F. K. *Discuss. Faraday Soc.* **1953**, *15*, 161.
(4) Franks, F.; Johnson, H. H. *Trans. Faraday Soc.* **1962**, 656.
(5) Bertrand, G. L.; Millero, F. J.; Wu, C.-H.; Hepler, L. G. *J. Phys. Chem.* **1966**, *70*, 699.
(6) Oakes, J. *J. Chem. Soc., Faraday Trans. II* **1973**, *69*, 1311.
(7) Coccia, A.; Indovina, P. I.; Podo, F.; Viti, V. *Chem. Phys.* **1975**, *7*, 30.
(8) Ben-Naim, A. *J. Chem. Phys.* **1977**, *67*, 4884.

0002-7863/88/1510-5246$01.50/0

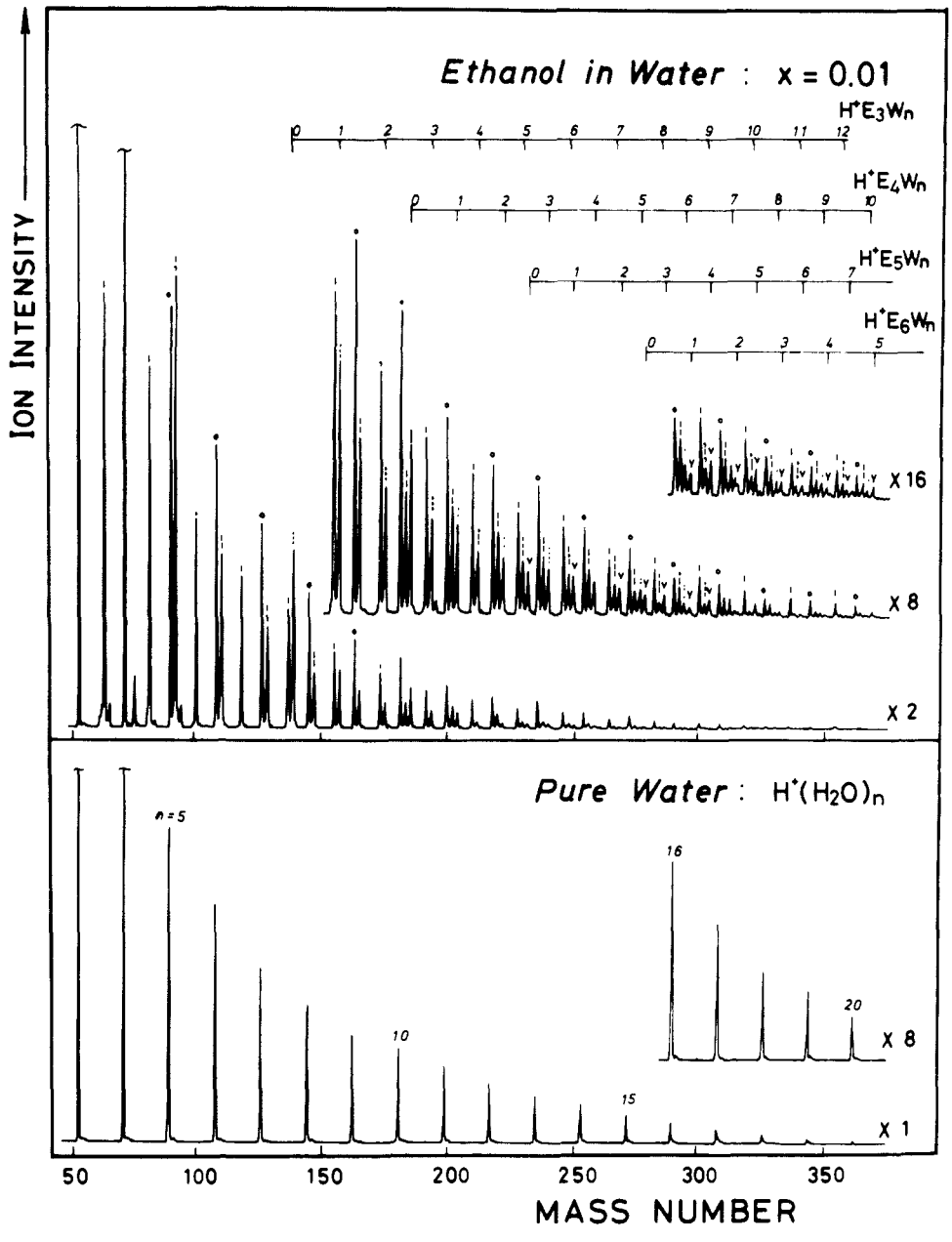

Figure 1. Mass spectra of cluster fragments of ethanol aqueous solution with x (ethanol molar fraction) = 0.01 (top) and those of pure water (bottom) at 35 °C. E and W represent C_2H_5OH and H_2O, respectively. Electron impact ionization energy = 40 eV.

a little smaller upon ionization.[1] Thus one must notice the following pathways: For $m \ll n$

$$(C_2H_5OH)_m(H_2O)_n \xrightarrow{e^-} H^+(C_2H_5OH)_m(H_2O)_{n-s-1} + OH + s(H_2O) \quad (1)$$

and for $m \gg n$

$$(C_2H_5OH)_m(H_2O)_n \xrightarrow{e^-} H^+(C_2H_5OH)_{m-t-1}(H_2O)_n + C_2H_5O + t(C_2H_5OH) \quad (2)$$

where s and t are most probably in the range of 1–3.[1,9] The small evaporation numbers are thought to originate from the relatively large hydrogen bond energy (5.4 kcal/mol for water)[10] and rather localized molecular orbitals in hydrogen bonding systems.[11,12]

Any water molecule in a cluster is bound to at least two sites so that more than 10 kcal/mol of excess energy is required to dissociate a water molecule. Localization of such a large energy at a hydrogen bond becomes less probable in larger clusters. This situation is very different for metal clusters and single molecules, where ionization is often accompanied by direct dissociation of atom–atom bond(s).

Small binary clusters with m values close to n are considered to follow reaction 2, since the ionization potential of ethanol (10.65 eV) is smaller than that of water (12.62 eV)[13] so that immediate charge transfer from H_2O^+ to the neighboring C_2H_5OH is expected to occur. In this paper, we neglect any information from clusters with fewer than 3 molecules for the discussion of cluster formation equilibria in solution. Information from large clusters is sufficiently reliable as long as one does not specify the cluster sizes (m and n) of parent clusters.

(9) Stace, A. J.; Moore, C. *J. Am. Chem. Soc.* **1983**, *105*, 1814.
(10) Curtiss, L. A.; Frurip, D. J.; Blander, M. *J. Chem. Phys.* **1979**, *71*, 2703.
(11) Tse, Y.-C.; Newton, M. D.; Allen, L. C. *Chem. Phys. Lett.* **1980**, *75*, 350.
(12) Frisch, M. J.; DelBene, J. E.; Binkley, J. S.; Schaefer, H. F., III *J. Chem. Phys.* **1986**, *84*, 2279.
(13) Levin, R. D.; Lias, S. G. *Ionization Potential and Appearance Potential Measurements (1971–1981)*; National Bureau of Standards: Washington DC, 1982.

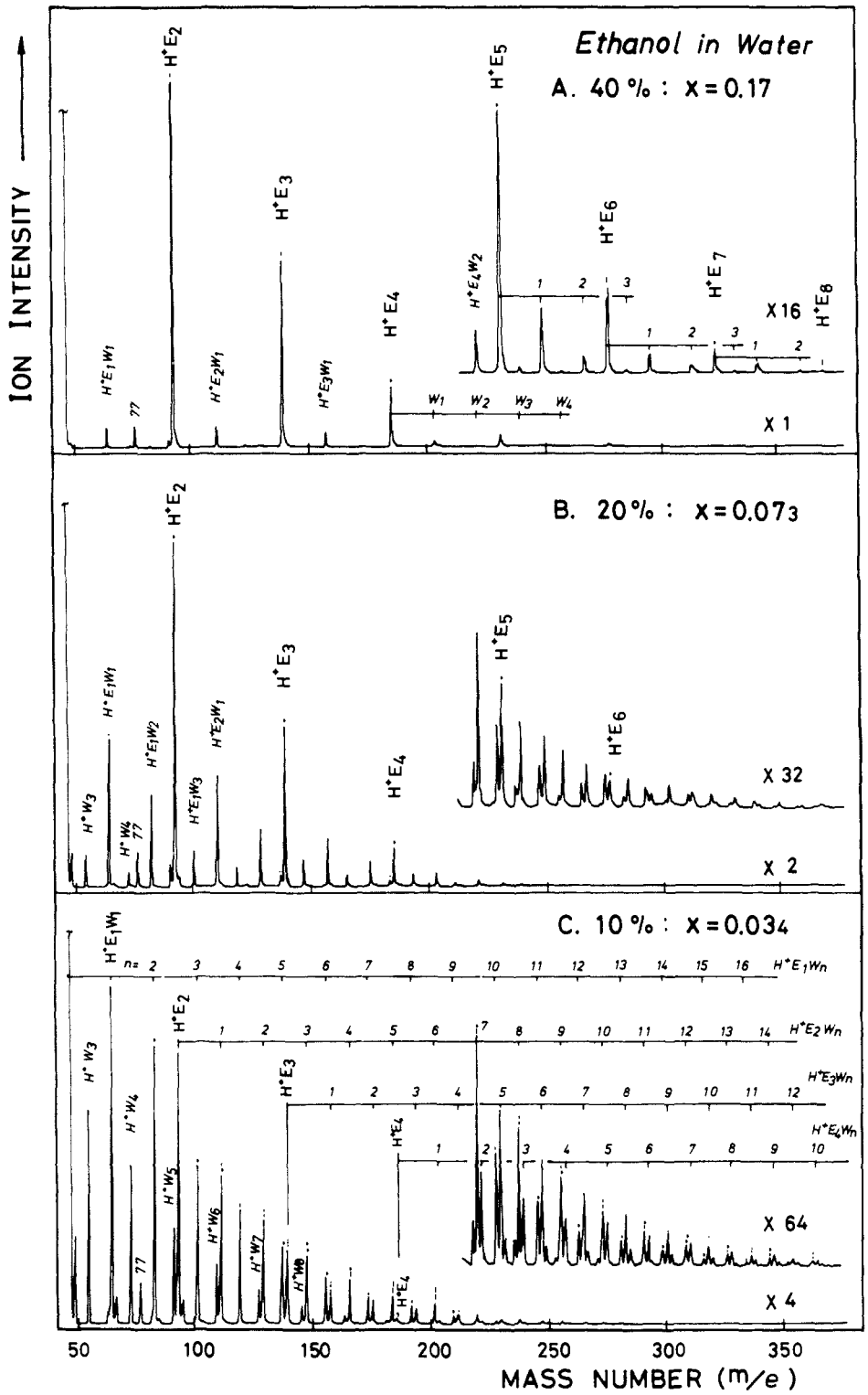

Figure 2. Mass spectral change of cluster fragments at three ethanol concentrations: (A) $x = 0.17$ (ethanol volume % = 40%), (B) $x = 0.073$ (20%), (C) $x = 0.034$ (10%). Temperature of liquid = 80 °C.

II. Experimental Section

The apparatus used in this study is the same as reported previously.[1] The nozzle is made of an injector needle (Hamilton type N731) which has an exit hole smaller than 50 μm. The nozzle–skimmer distance was fixed at about 2.5 mm in order to avoid collisional effects on the cluster distribution. The temperature of the needle was measured at a position 4 mm behind the liquid-nozzle head with a copper–constantan thermocouple. This temperature was found to be ~40 °C higher than the temperature of the liquid at a liquid flow rate of 1.4 μL/s. This temperature drop increased for a faster flow rate of liquid. Sample solution was injected through a liquid chromatograph pump with a constant flow rate. The liquid jet flow was surrounded by argon gas flow so that the divergence angle of the generated mist flow was narrowed. The stagnation pressure of argon in the outer gas nozzle was ~100 Torr. The vacuum in the expansion chamber was 0.24 ± 0.02 Torr. However, the pressure around the nozzle was expected to be much higher because of the presence of outergas-flow around the liquid jet. This flow may keep the mist stable in a certain period. The second chamber between the two skimmers was evacuated at pressures lower than 5×10^{-3} Torr and the detection chamber was lower than 1×10^{-7} Torr. The expansion of mist particles forming clusters occurs mainly in the second chamber between the two skimmers. The first skimmer skims the mist flow and the second one extracts the clusters fragmented by adiabatic expansion of the mist particles in the sufficiently low density area. The pressure applied to the liquid in the stainless steel pipe was measured by a Bourdon type pressure

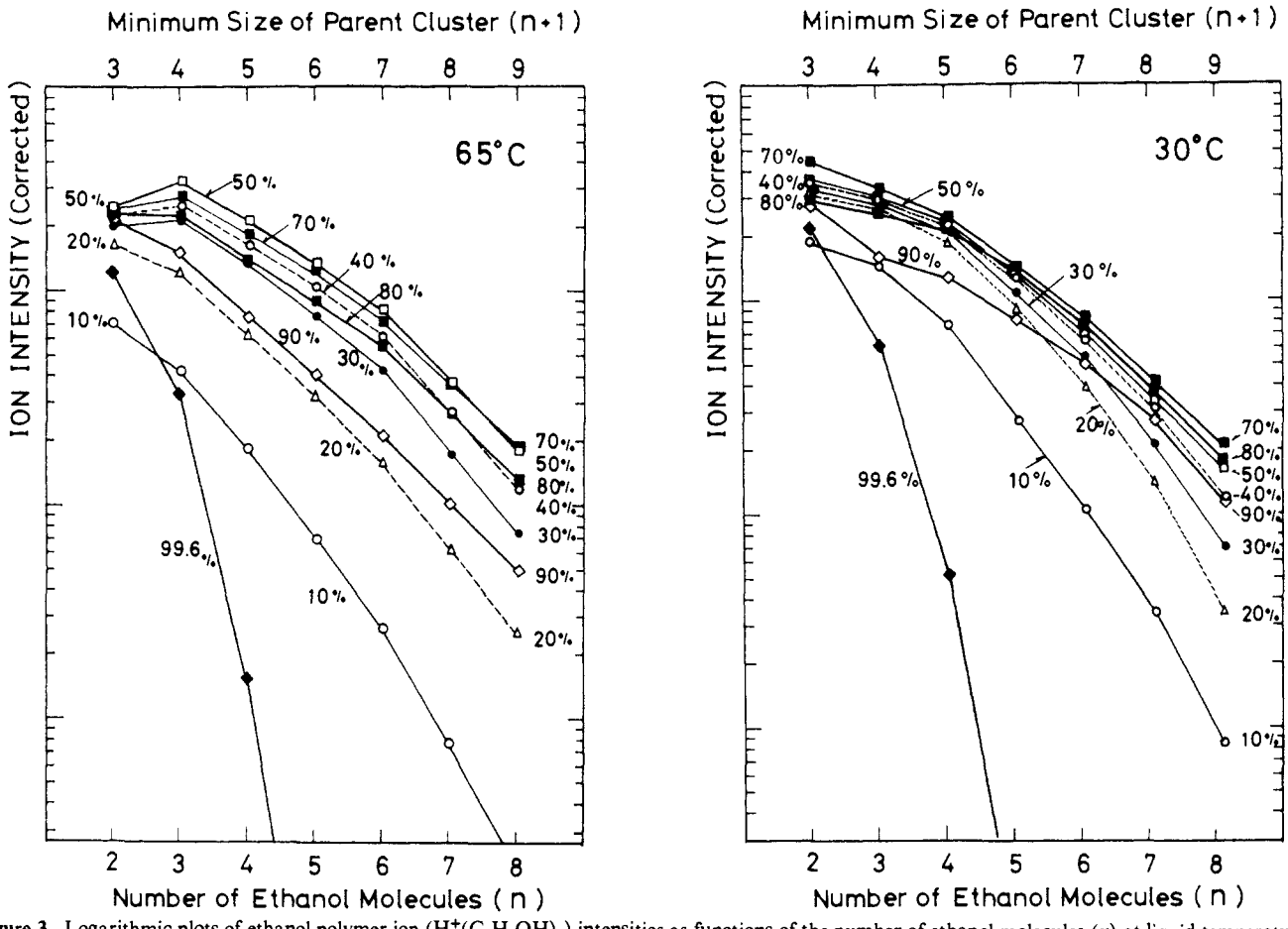

Figure 3. Logarithmic plots of ethanol polymer ion ($H^+(C_2H_5OH)_n$) intensities as functions of the number of ethanol molecules (n) at liquid temperature of 65 °C (left) and 30 °C (right). Ethanol concentrations are given by vol % and correspond to the mole fractions as follows: x = 0.034 at 10%, 20% ⇒ 0.072, 30% ⇒ 0.12, 40% ⇒ 0.17, 50% ⇒ 0.24, 60% ⇒ 0.32, 70% ⇒ 0.42, 80% ⇒ 0.56, 90% ⇒ 0.74, and x = 0.999 at 99.6%.

gage (Shinagawa Sokki, model LCG50D) through a three-way junction at the entrance to the vacuum chamber. For a flow rate of 1.4 μL/s, the liquid pressure was about 3 atm.

In order to know the temperature of the liquid from which the final molecular configuration originated, we observed the lower critical solution temperature (LCST, 49 °C) and the upper critical solution temperature (UCST, 128 °C) of an aqueous solution of 5% 2-butoxyethanol under the same expansion conditions. This solution showed phase separation between 49 and 128 °C.[1]

A quadrupole mass spectrometer equipped with an electron impact ionizer (ANELVA AGA-360) was situated perpendicular to the beam direction 8 cm downstream from the nozzle. Mass dependence of the spectrometer (ion transmission and sensitivity of the detector) was calibrated by measuring the spectral pattern of perfluoro-*n*-hexane at an electron energy of 20 eV.[1] Output from an electrometer was accumulated for 128 scans in a Nicolet 1174 signal averager.

III. Results

Cluster Beam Density. Since the cluster beam is generated continuously from a liquid jet at a flow rate of 1.4 μL/s, the beam density becomes very high in a single chamber experiment. However, electron impact ionization should be carried out at a beam density where the contribution of ion exchange reactions to the cluster ion distribution is negligibly small. Our ionizer was situated 8 cm downstream from the nozzle across the doubly differential pumping stages. The distance from the nozzle to the second skimmer is 1.6 ± 0.2 cm. The cluster density was measured by using an ion gauge and a mass spectrometer. In order to calibrate the signal intensity of the mass spectrometer for N_2 and the beam constituents, N_2, H_2O, and acetone were introduced independently at a pressure of 2×10^{-7} Torr and their signal levels (at this pressure) were used as the measures of the partial pressures of the beam components. After evacuating these standard gases, a cluster beam was produced from an acetone–water (molar ratio = 1:5) mixture and its mass spectrum was recorded under the same condition of the detector system. The strongest ion was H_2O^+ whose intensity gave a partial pressure of 1.0×10^{-5} Torr. The cluster ions were mostly pure water clusters $H^+(H_2O)_n$, and their intensities were less than 2% of the H_2O^+ signal. The intensity of $H^+(H_2O)_4$ was 1×10^{-2} that of H_2O^+.

The same experiment was also done for the ethanol–water (1:5) mixture, which showed the strongest peak of H_2O^+ in the mass spectrum of the beam. The intensity of H_2O^+ was equivalent to a partial pressure of 0.8×10^{-5} Torr. Thus the beam density was estimated to be $\lesssim 2 \times 10^{-5}$ Torr and the cluster density was of the order of 10^{-6} Torr. The latter value is in good agreement with the water cluster intensities relative to that of the background N_2 signal seen in Figure 2 of ref 1. Namely, the $H^+(H_2O)_2$ peak is 12 times as strong as the signal of the background N_2 which has a partial pressure of $\sim 5 \times 10^{-8}$ Torr. The acetone–water (1:5) mixture produced also the acetone hydrate ions $H^+(CH_3COCH_3)(H_2O)_n$ whose intensities were less than 10% of the $H^+(H_2O)_{n+1}$ signals. As shown in the following section, the ethanol–water mixtures with ethanol mole fractions larger than 0.18 produced mostly pure ethanol clusters. This is a remarkable contrast with the clusters produced from the acetone–water mixture. The proton affinity of acetone (≥195 kcal/mol) is larger than that of ethanol (186 kcal/mol).[14] If the ion–molecule reactions such as the proton transfer from $H^+(H_2O)_n$ to an acetone occur seriously in the ionizer, pure water cluster ions in the acetone–water system should be much less than those in the ethanol–water system. However, the observed result is just the opposite and strongly demonstrates that the contribution of the proton transfer (from $H^+(H_2O)_n$ to the solute molecules) to the observed cluster ion distribution is negligible with the present beam condition. This conclusion was also supported by the ion density

(14) Lias, S. G.; Ausloos, P. *Ion–Molecule Reactions*; American Chemical Society: Washington, DC, 1975; 91–92.

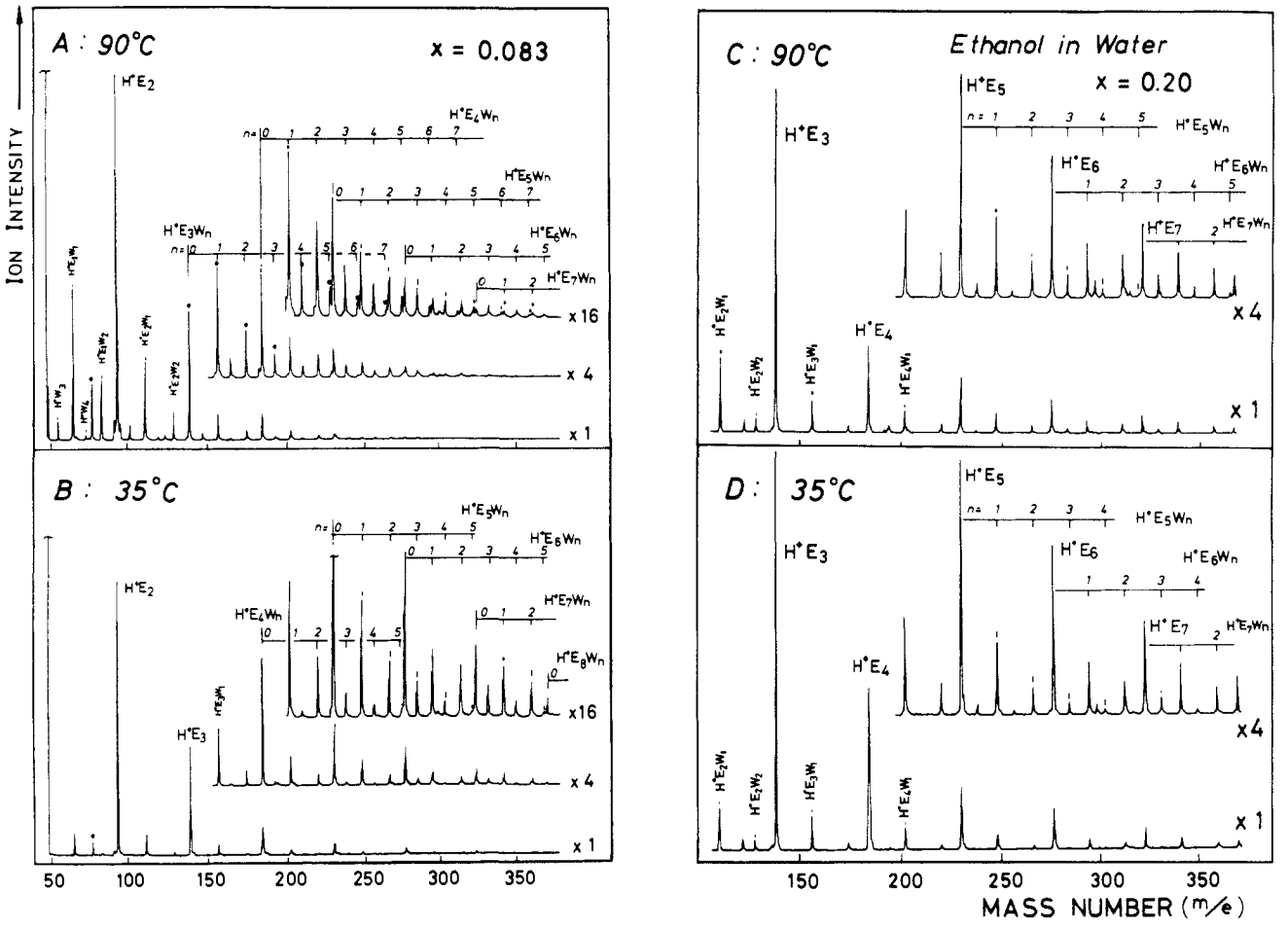

Figure 4. Temperature dependence of mass spectral pattern of ethanol aqueous solutions at two concentrations: $x = 0.083$ (A and B), and $x = 0.20$ (C and D).

dependence of the cluster distribution. Upon the increase of the filament emission current of the ionizer from 10 to 200 μA, the cluster beams of the acetone–water and ethanol–water mixtures showed no significant spectral change.

Concentration Dependence of Cluster Distribution. As reported previously,[1] the mass spectral intensities of both ethanol monomer–hydrate and dimer–hydrate clusters were directly proportional to the ethanol molar fractions of the binary solutions with $x \leq 0.02$. However, the intensities relative to those of pure water clusters (with the same molecular numbers) are more than 5 times as strong as those expected by a stochastic model,[1] which indicates higher stability of ethanol monomer and polymer hydrate clusters in aqueous environments. Figure 1 shows the mass spectrum of ethanol–water (1:100) solution at 35 °C along with the cluster spectrum of pure water in the bottom. Despite the relatively small mole fraction of ethanol (~0.01), very strong water sequences of monomer and dimer hydrates and strong sequences of trimer, tetramer, pentamer, and even hexamer hydrates can be clearly seen. The presence of so many species makes the spectrum very complicated. When this spectrum is compared with the spectra shown in Figure 11 of ref 1, one may find that the higher ethanol polymers are dissociated remarkably with increasing temperature. Figure 2 shows mass spectral changes of the cluster beams generated from the ethanol aqueous solution with three different solute concentrations at a liquid temperature 80 °C and liquid pressure of 3 bar. Because of the large difference in the sensitivity at low masses (down to mass 47) and at high mass side (up to mass 370), cluster signals show rather steep intensity decreasing with increasing cluster size. The corrected intensities of the high mass signals, however, are much stronger than those appearing in the spectra. The top spectrum is dissimilar to the bottom one. The main sequence of the bottom spectrum is composed of water progressions with a mass interval of 18, while that of the top spectrum has ethanol progressions with a mass interval of 46. The spectral feature seen in the top spectrum was usually observed for the solutions with ethanol mole fractions larger than 0.12. It consists of the $H^+(C_2H_5OH)_m$ sequence accompanied with weak signals of the hydrated species $H^+(C_2H_5OH)_m(H_2O)_n$ (n = 1, and 2).

Temperature Dependence of Association Equilibrium. The intensities of the ethanol polymer signals are highly dependent on the temperature of the binary solutions and also change with the concentration of ethanol. Figure 3 shows the concentration dependence of the polymer intensities at 65 and 30 °C where the observed ion intensities (corrected for the mass dependent detector sensitivity)[1] are plotted as a function of the number of ethanol molecules. The polymer sequence (n = 2, 3, ..., 6) observed at the indicated concentration is connected by a line whose slope shows the relative size of the average polymer at the given concentration. At 65 °C, the strongest polymer signals were observed at an ethanol concentration of 50 vol % ($x = 0.24$). At 30 °C, the solution with 70 vol % of the ethanol ($x = 0.42$) gave the strongest polymer sequences. Ethanol polymer dissociation became active with increasing temperature, which is roughly independent of solute concentration. The 50% solution showed strongest polymer intensities at 65 °C, and the 40% solution at 80 °C, although the absolute intensities decreased upon warming. At 30 °C, all the solutions with ethanol concentration of 40–80% (x = 0.17–0.56) provided quite similar spectral patterns of the polymer signals; this indicates the similarity of average polymer sizes despite the variation of ethanol to water ratio in this region.

It is reasonable that thinner solutions showed weaker signals of higher polymers, while it was unexpected that the purest alcohol (99.6%, $x = 0.999$) revealed drastically reduced intensities of the higher polymer signals. The trimer signal of the 10% solution ($x = 0.034$) is 2.7 times as strong as that of the 99.6% solution,

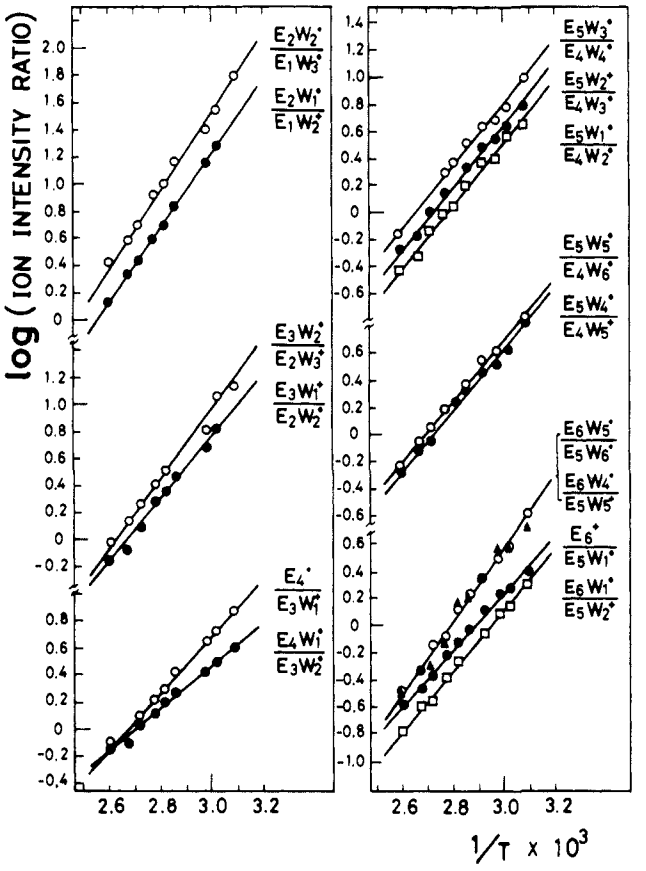

Figure 5. Logarithmic plots of intensity ratios $[H^+(C_2H_5OH)_m(H_2O)_{n-1}]/[H^+(C_2H_5OH)_{m-1}(H_2O)_n]$ as functions of $1/T$ observed for an ethanol aqueous solution with $x = 0.083$.

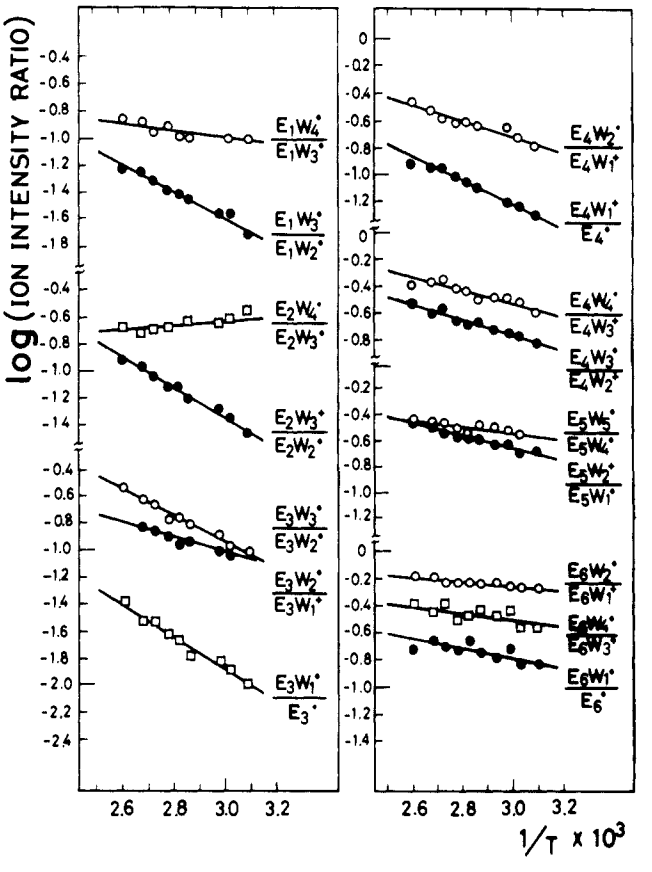

Figure 6. Logarithmic plots of intensity ratios $[H^+(C_2H_5OH)_m(H_2O)_n]/[H^+(C_2H_5OH)_m(H_2O)_{n-1}]$ as functions of $1/T$ observed for an ethanol aqueous solution with $x = 0.083$.

and the tetramer signal of the more dilute solution (10%) is 16 times as intense as that of the most concentrated solution (99.6%) at 30 °C. *These facts indicate that the presence of water molecules is indispensable to the growth of ethanol polymer chains.*

As shown in the previous report,[1] ethanol association in dilute solutions exhibited a drastic temperature dependence. This trend was observed for the solution with ethanol mole fractions of less than 0.12 (30 vol %). Figure 4 displays the temperature dependence of the spectral patterns at the ethanol mole fractions of 0.08 and 0.20. The thinner system ($x = 0.08$) showed a clear temperature change: at the higher temperature (90 °C), higher ethanol polymers were dissociated producing smaller polymers accompanied with more water molecules. On the contrary, the thicker solution ($x = 0.20$) showed little temperature dependence of the spectral pattern although higher polymers were dissociated to some extent at higher temperatures. The nature of the solution appeared to change at some concentration in the region of x = 0.083–0.42.

The ethanol polymer distributions shown in Figure 3 suggest that the polymer evolution–dissociation equilibrium is not so sensitive to the increase of ethanol mole fraction in the region of x = 0.17–0.42 (40–70%) where the intensity ratio $[H^+(C_2H_5OH)_m]/[H^+(C_2H_5OH)_{m-1}]$ is nearly constant for m = 3–8. In aqueous systems, the following equilibria should be considered:

$$(C_2H_5OH)_{m-1}(H_2O)_n + C_2H_5OH \overset{K_{m,n}}{\rightleftharpoons} (C_2H_5OH)_m(H_2O)_{n-1} + H_2O \quad (3)$$

where

$$K_{m,n} = \frac{[(C_2H_5OH)_m(H_2O)_{n-1}]}{[(C_2H_5OH)_{m-1}(H_2O)_n]} \frac{[H_2O]}{[C_2H_5OH]} \quad (4)$$

Figure 5 shows the logarithmic plots of the intensity ratios, $[H^+(C_2H_5OH)_m(H_2O)_{n-1}]/[H^+(C_2H_5OH)_{m-1}(H_2O)_n]$ (m = 2–6 and n = 1–4), against T^{-1} for the solution with $x = 0.083$. All the plots are linear in the temperature range 50–110 °C. This type of plot is the so-called van't Hoff plot whose slope value gives the enthalpy change of the molecular exchange process (reaction 3) between the parent species of the observed ions.[1]

Figure 6 displays the van't Hoff plots of the ratios $[H^+(C_2H_5OH)_m(H_2O)_n]/[H^+(C_2H_5OH)_m(H_2O)_{n-1}]$ for m = 1–6 and n = 1–4. Except for the ratio with $m = 2$ and $n = 4$, all the plots exhibited negative slopes indicating that the formation of higher hydrates is endothermic in contrast to the exothermic ethanol association processes (Figure 5). The obtained values of the enthalpy changes for the exchange and the evolution–dissociation processes are summarized in Figure 7. The result must be compared with the enthalpy changes for a much diluted solution with $x = 0.01$ (Figure 13 of ref 1). Although some parts are different in the present system ($x = 0.08$), the average enthalpy change for the overall processes remains to be 4.5 kcal/mol, which is the same as the average value in the diluted system. Thus the essential nature of the association processes appeared to be unchanged with increasing ethanol concentration up to $x = 0.08$. It must be also noticed that the water attachment processes in the diluted system were also endothermic for the small clusters with $m + n \leq 10$.

The equilibrium constant $K_{m,n}$ depends on the hydration number n. In the stochastic model,[1] this constant is proportional to the hydration number. We proposed using the alternative constants κ_1 and κ_2 which are independent on the hydration numbers and related to the equilibrium constants by the following equation: $\kappa_m = mK_{m,n}/n$ (m = 1 and 2). For the solution with $x = 0.01$, $\kappa_1 = 5.5 \pm 0.6$ and $\kappa_2 = 8.0 \pm 0.8$ at 65 °C, and at 35 °C $\kappa_1 = 13.7 \pm 1.0$ and $\kappa_2 = 19 \pm 2$. Temperature dependence is very large for these exchange processes and at low temperatures the equilibria shift toward attachment of an ethanol molecule to a cluster in replacement of a water molecule. For a cluster with a hydration number of 10, $K_{1,10}$ becomes 137 and $K_{2,10}$ is 95 at

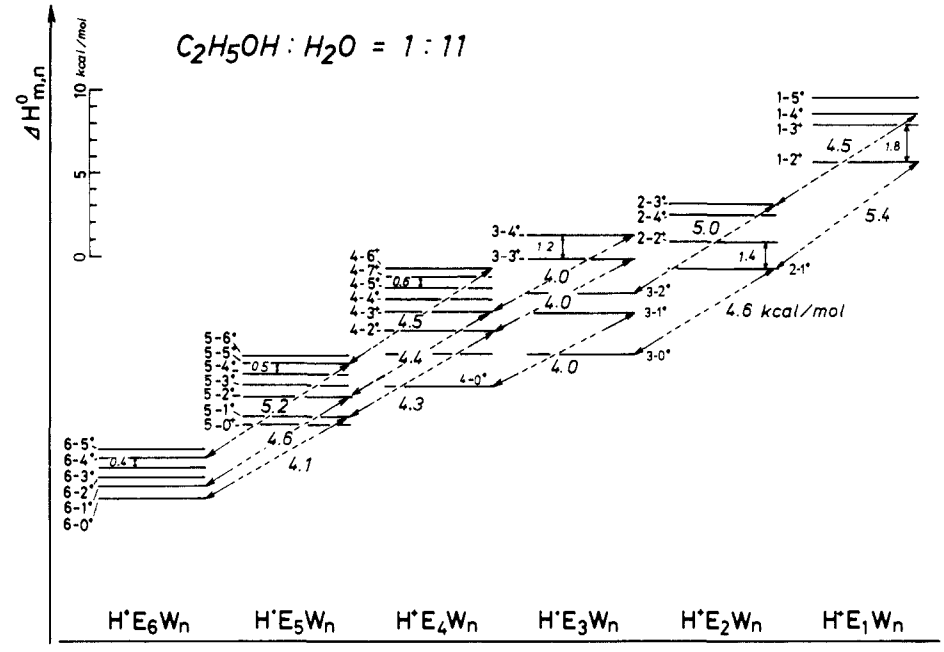

Figure 7. Enthalpy changes for molecular exchange processes (eq 3, shown by dotted arrows) in an ethanol–water (1:11, $x = 0.03$) solution. Errors for the respective values are ±0.5 kcal/mol.

35 °C. These values indicate that even for the ethanol molar ratio of 1/100, the concentrations of $C_2H_5OH(H_2O)_{9+s}$ and $(C_2H_5OH)_2(H_2O)_{8+s}$ ($s = 1$ or 2, most probably) are of the same order as $(H_2O)_{10}$ at 35 °C. Namely, a greater part of water molecules are bound to ethanol monomer and polymers forming hydrate clusters $(C_2H_5OH)_m(H_2O)_n$.

Saturation of Polymer Formation Equilibria. Logarithms of the intensity ratio $[H^+(C_2H_5OH)_m(H_2O)_{n-1}]/[H^+(C_2H_5OH)_{m-1}(H_2O)_n]$ were plotted as a logarithmic function of molar ratio of total ethanol to total water molecules in Figure 8. If the concentration ratio of the free ethanol to the free water molecules in the solution is proportional to the molar ratio of total solute to total solvent molecules, the log–log plots provide the slope of unity according to eq 4. The equilibrium constants, $K_{m,n}$ for various m and n, are constant only for solutions that provide a slope of unity for the plots. For $x \geq 0.18$, all the intensity ratios gave slope values lower than 0.7. This corresponds to the observation shown in Figure 3 that the intensity ratios of the ethanol polymers ($[H^+(C_2H_5OH)_m]/[H^+(C_2H_5OH)_{m-1}]$) are nearly constant for the solutions in this concentration range. Apparently the ratio of $[C_2H_5OH]/[H_2O]$ is not proportional to the molar ratio of total ethanol to total water molecules in the concentrated solutions with $x \geq 0.18$. According to the change in slope of the various cluster intensity ratios, the solutions were classified into four concentration regions, (a) to (d). In region (a) with $x \leq 0.08$, the concentration ratio of free solute to free solvent molecules is proportional to the molar ratio of total solute to total solvent molecules and the nature of the solution in this region is characterized as essentially aqueous, although pure water cluster formation is highly unfavorable at the concentrations of $x > 0.04$. At the boundary between region (b) and region (c), the formation of hydrogen bonding networks becomes almost saturated and both ethanol and water molecules are bound to the hydrogen bonding networks. This results in the deficit of free water molecules relative to free alcohol molecules at higher ethanol concentrations. Thus in region (c) the molar ratio of the free molecules $[C_2H_5OH]/[H_2O]$ is no longer proportional to the ratio of total alcohol to total water molecules.

IV. Ab Initio Calculation of Dimers

In the past decade, ab initio molecular orbital theory has been shown capable of giving a reliable account of a variety of hydrogen-bonded interactions.[11,12,15-18] In order to get the best knowledge of the gas-phase interaction energies, we carried out ab initio calculations of the hydrogen-bonded dimers formed from water, ethanol, and methanol by using the GAUSSIAN 82 program[19] on a HITAC M680H computer. For all calculations, Pople's 6-31G** basis set[20] was used to produce reliable hydrogen-bonding energies. All of the dimer geometries were optimized by using the energy gradient method[21] with respect to all geometrical degrees of freedom. As pointed out by Dill et al.[15] and Tse et al.,[11] a fully reliable computational model requires 3d polarization functions as well as an extended valence s,p basis on the heavy atoms. The 6-31G** basis set contains a single set of gaussian p-type functions for each hydrogen and helium.

Figure 9 shows the optimized geometries of the water–ethanol and ethanol–ethanol dimers. The calculated bond energies (D_e) of seven different dimers are given in Table I. The values for the water and methanol systems are very close to the values calculated on the 6-31G* basis set by Tse et al.[21] Although a slightly larger stabilization energy was obtained for the water–ethanol dimer, HO–H- -OHC_2H_5, all bond energies are in the range of 5.4–5.85 kcal/mol. One must note that *the ethanol–ethanol interaction is nearly the same as that of the water–water pair.* This is important for understanding the stability of ethanol polymers in aqueous solutions.

V. Discussion

Comparison of the Results with NMR Studies and Thermodynamic Properties. The present mass spectrometric analysis of the solute and solvent association shows good agreement with the various data obtained by other methods.[2-7,9,22,23] High-resolution NMR spectroscopy is a powerful approach providing information at a local molecular level since hydrogen-bonding strength (or

(15) Dill, J. D.; Allen, L. C.; Topp, W. C.; Pople, J. A. *J. Am. Chem. Soc.* **1975**, *97*, 7220.
(16) Kollman, P. A. *Modern Theoretical Chemistry*; Schaefer, H. F., III, Ed.; Plenum: New York, 1977; Vol. 4.
(17) Umeyama, H.; Morokuma, K. *J. Am. Chem. Soc.* **1977**, *99*, 1316.
(18) Newton, M. D. *J. Chem. Phys.* **1977**, *67*, 5535.
(19) Binkley, J. S.; Frish, J. M.; DeFrees, D. J.; Raghavachri, K.; Whiteside, R. A.; Schlegel, H. B.; Fluder, E. M.; Pople, J. A., Carnegie-Mellon University, Pittsburgh, PA 15213 (a library program of the Computer Center of Institute for Molecular Science, Okazaki, 1985).
(20) Haribaran, P. C.; Pople, J. A. *Theor. Chim. Acta* **1973**, *28*, 213.
(21) Komornicki, A.; Ishida, K.; Morokuma, K.; Ditchfield, R.; Conrad, M. *Chem. Phys. Lett.* **1977**, *45*, 595.
(22) Rüterjans, H. H.; Scheraga, H. A. *J. Chem. Phys.* **1966**, *45*, 3296.
(23) Laiken, N.; Némethy, G. *J. Phys. Chem.* **1970**, *74*, 3501.

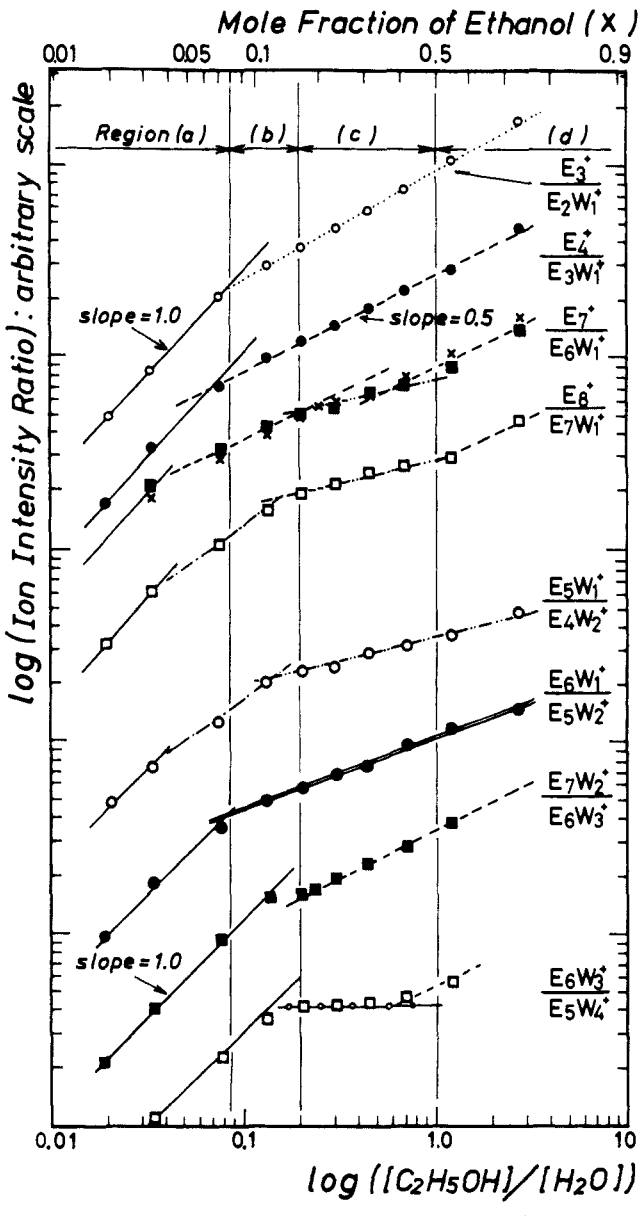

Figure 8. Log–log plots of the intensity ratio $[H^+(C_2H_5OH)_m(H_2O)_{n-1}]/[H^+(C_2H_5OH)_{m-1}(H_2O)_n]$ against molar ratios of total ethanol to total water molecules ($x/(1-x) = x_E/x_W$). Solid lines present a slope of unity indicating that the ethanol polymer chains grow in proportional to the molar ratio x_E/x_W.

lifetimes of hydrogen-bonded complexes) can be derived from chemical shift measurements. Coccia et al. studied chemical shifts of the hydroxy signals in water–ethanol mixtures over the entire composition range of the two cosolvents.[7] Figure 10 shows their result obtained at 100 MHz and 20 °C. When ethanol was added to water, the single sharp hydroxy signal of water was first shifted toward lower fields, reaching a minimum 5.5 Hz deep at $x = 0.08$. This chemical shift remained nearly constant up to $x = 0.20$. Above $x = 0.20$, this signal shifted linearly with increasing x toward higher fields. This indicated that the hydrogen-bonding lifetimes of water molecules became much shorter at higher ethanol concentration. The present mass spectrometric data have suggested that, in region (a) with $x \leq 0.08$, free water molecules tend to attach to ethanol hydrated clusters rather than to pure water clusters. This trend was shown numerically by the equilibrium constants ($K_{1,n}$ and $K_{2,n}$) and by the exothermic enthalpy changes of the exchange processes of eq 3 as exhibited in Figure 7. Actually the water cluster signals of $H^+(H_2O)_n$ are hardly seen in the spectrum of the beam with $x = 0.08$ (Figure 4A and 4B). Above $x = 0.08$, the spectral pattern changed gradually and hydrated cluster signals became fainter with increasing x. At the

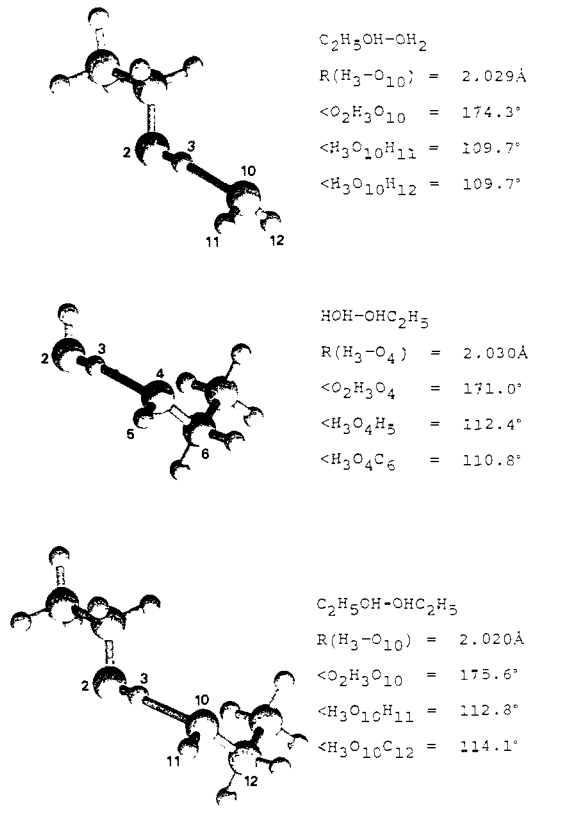

Figure 9. HF/6-31G** optimized geometries of water–ethanol and ethanol–ethanol dimers. Only the hydrogen-bonding parameters are shown, although full gradient optimization was carried out.

Table I. 6-31G** Calculation of Hydrogen Bond Energies for Dimers

proton donor	proton acceptor	D_e	(kcal/mol)
HOH	OH_2	5.54	(obsd = 5.4)[9]
	$OHCH_3$	5.42	
	OHC_2H_5	5.85	
C_2H_5OH	OH_2	5.44	
	OHC_2H_5	5.66	
CH_3OH	OH_2	5.52	
	$OHCH_3$	5.42	

saturation point of $x = 0.08$, the hydrogen bonds of water molecules become most stable as revealed by the chemical shift measurement. This is clearly attributed to the nearly complete hydration of ethanol molecules at this concentration. Ben-Naim found that the average affinity of ethanol to another ethanol showed a maximum at $x \approx 0.08$.[9] This means that ethanol molecules are located very close to each other at this concentration.

As pointed out by Franks and Ives,[2] all experimental evidence showed that no more than two hydrogen bonds are formed for an alcohol molecule, each oxygen acting once as hydrogen donor and once as hydrogen acceptor. This was attributed to the equality of "give-and-take" which is due to the essentially cooperative nature of hydrogen bonding. Steric effects of the organic group may also preclude three-dimensional association of ethanol molecules. This situation is very different from the formation of hydrogen-bonding networks among water molecules which are essentially three dimensional due to the four hydrogen bonds of one water molecule. The presence of excess ethanol molecules at $x > 0.08$, therefore, destroys the three-dimensional networks producing nonbonded hydrogen atoms and lone-pair electrons, which increases the expanded molecular space due to the repulsive interactions between the hydrogen atoms. The partial molar volume (V_2) of ethanol in aqueous mixture showed a sharp minimum at $x = 0.08$ indicating closest contact of an ethanol molecule with surrounding molecules.[3,4] Mass spectrometrically, the ethanol polymer sequence $H^+(C_2H_5OH)_n$ ($n = 2, 3, \ldots$) is the

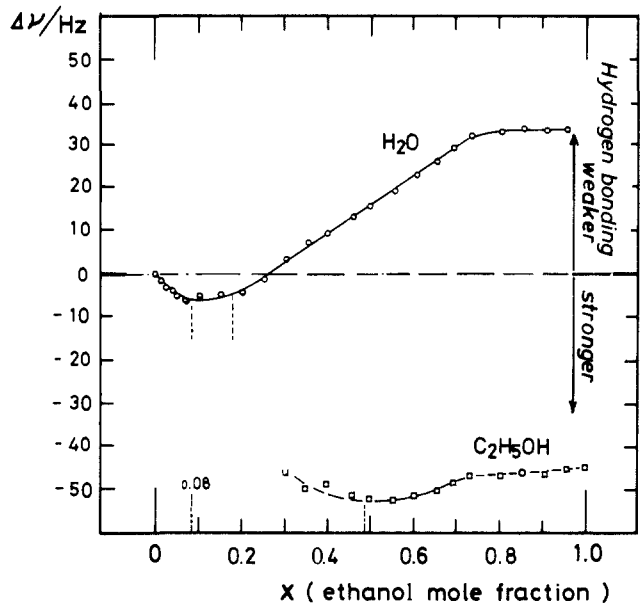

Figure 10. Chemical shifts of hydroxy signals in ethanol–water mixtures relative to that of pure water (data taken from ref 7 by Coccia et al.).

main cluster signal at this concentration. Hydrated cluster signals are not so strong as those of the pure ethanol polymers at 35 °C. Enthalpy changes for the water addition to ethanol monomer or polymers are endothermic for small numbers of waters ($n \leq 6$) in the mixture with $x = 0.08$ (Figure 7). This is most probably due to the fact that *the water attachment involves the breaking of an ethanol–ethanol bond which is highly stabilized in the aqueous system.* Thus the hydration number (n) of the observed ion, $H^+(C_2H_5OH)_m(H_2O)_n$, is smaller than the polymer size (m) at this concentration.

Structure of Ethanol–Water Clusters: Ethanol Chain Formation and Hydrophobic Hydration. On the basis of the present mass spectrometric data and the ab initio calculation of the optimized ethanol dimer geometry as well as the NMR and thermodynamic properties, we present a model of ethanol–water clusters as illustrated in Figure 11. The most stable cluster form in this binary system is ascribed to linear chains of ethanol polymers based on the give-and-take equality of the oxygen atom of ethanol.[2,24] This chain must situate the neighboring ethyl groups in a helical configuration to keep the independence of each ethyl group. The ethanol CH_3 group is oriented toward the oxygen atoms of the neighboring molecule in Figure 11. However, in an aqueous environment, interstitial water molecule(s) may change the direction of the CH_3 group due to strong hydration. This model is essentially the same as the Kempter–Mecke type oligomer model[25] expressed by an infinite series of $(C_2H_5OH)_n$. In sufficiently water rich solutions with $x < 0.04$, water molecules form strong hydrogen-bonding shells around an ethyl group core as revealed by the strong and long water sequences accompanying ethanol polymers (Figures 1 and 2C). This water shell model is based on the observation that the enthalpy change for the formation of monomer hydrates from pure water clusters is nearly the same as that for the dimer hydrate formation from the monomer hydrate clusters (Figure 13 of ref 1). Namely, the addition of one ethanol molecule to pure water clusters $(H_2O)_n$ or to hydrate clusters $(C_2H_5OH)_m(H_2O)_n$ produced a nearly constant enthalpy decrease ($\Delta H° \approx 4.5$ kcal/mol for $m = 0$–2). As stated in ref 1, the observed trend of ethanol–ethanol association is therefore attributed to the hydrophobic hydration of an ethyl group of an ethanol molecule in aqueous environment. Since the ethanol polymer signals become highly dominant at $x \geq 0.07$, the ethanol–ethanol bond must be stabilized already at $x = 0.01$. The trunk of this alcohol hydrogen-bonding chain will be attached by

(24) Fletcher, A. N.; Heller, C. A. *J. Phys. Chem.* **1967**, *71*, 3742.
(25) Marcus, Y. *Introduction to Liquid State Chemistry*; John-Wiley & Sons: New York, 1977; Section 5.2.4.

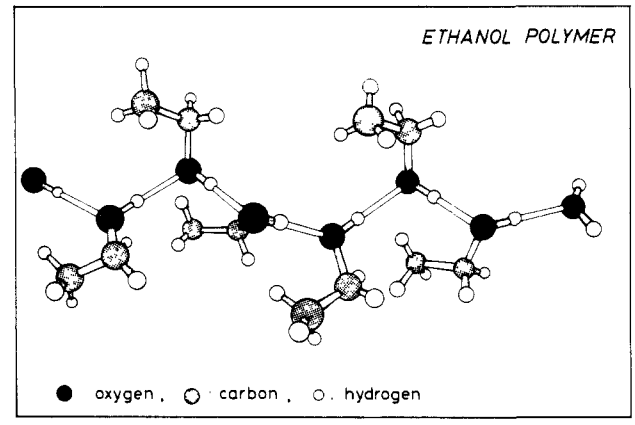

Figure 11. A model of an ethanol polymer with water molecules at the ends. Relative configuration of ethanol is obtained from the ab initio calculation of the optimized ethanol dimer geometry so that the CH_3 groups are located close to the oxygen atoms of neighboring ethanol molecules. In a water rich environment, the direction of the ethyl groups may be largely changed due to strong hydrophobic hydration around the ethyl groups.

helically oriented ice balls which have the cores of ethyl groups protruding from the chain.

The values of κ_1 and κ_2 in ref 1 showed that the hydration shells of ethanol are as strong as those of acetic acid. This hydration shell, however, does not remain stable in solutions with $x > 0.08$ at temperatures below 35 °C. The solutions with $x > 0.04$ showed stronger signals from pure ethanol polymers than from hydrated species. This indicates that, in the region of $x > 0.04$, water molecules surrounding ethyl groups do not form strong shells but may be only orientationally ordered for some periods. Close location of the two alkyl groups may destroy the formation of water shells. In this case, water molecules may just act as "fillers" that stabilize the ethanol polymer chains. For $x \geq 0.05$, the average number of water molecules per ethanol molecule falls below 20. Twenty water molecules can form a pentagonal dodecahedral cage; this is the minimum size of three-dimensional water shells.[26-30] Thus, if the average water number becomes smaller than 20, water molecules could not make any rigid cage and may remain weakly interacting with alkyl groups and with other water molecules. Since the formation of an ethanol chain produces large local fields, it could be necessary to have water fillers to compensate for the local potential anisotropy.

As shown by Figure 3, the signals of the higher ethanol polymers ($n > 4$) fall drastically for the 99.9% ethanol solution. Long ethanol chains are unstable in pure alcoholic environments. At 30 °C, the highest stability of ethanol polymers was obtained for the 70% ethanol solution ($x = 0.42$). This means that the equivalent mole fraction of water molecules is required to stabilize the ethanol chains. One must note that at $x \approx 0.42$ the average affinity of alcohol to water is at a minimum[8] and the excess Gibbs free energy of mixing (ΔG^E) reaches a maximum (Figure 2 of ref 2). The latter comes from a large decrease of the excess entropy of mixing. The formation of long ethanol chains most abundantly at this concentration is in good agreement with these and other observations.[5]

Between the two singular concentrations of $x = 0.08$ and 0.42, there is another important mixing point. At $x \simeq 0.18$, ethanol and water molecules combine to form the most stable and fully saturated clusters (Figure 8). The excess enthalpy change ΔH^M shows a minimum at $x \approx 0.18$ (Figure 2 of ref 2), which indicates that total intermolecular interaction becomes largest at this

(26) van der Waals, J. H.; Platteeuw, J. C. *Adv. Chem. Phys.* **1959**, *2*, 1.
(27) Kassner, J. L.; Hagen, D. E. *J. Chem.* Phys. **1976**, *64*, 1860.
(28) Hermann, V.; Kay, B. D.; Castleman, A. W., Jr. *Chem. Phys.* **1982**, *72*, 185.
(29) Shinohara, H.; Nagashima, U.; Tanaka, H.; Nishi, N. *J. Chem. Phys.* **1985**, *83*, 4183.
(30) Nagashima, U.; Shinohara, H.; Nishi, N.; Tanaka, H. *J. Chem. Phys.* **1986**, *84*, 209.

concentration. It is also reported that the viscosity reaches its maximum value at $x = 0.22$.[31] The cluster distribution does not change so much in region c ($0.18 \leq x \leq 0.5$) for both the increases of alcohol concentration and liquid temperature (Figure 4C and 4D). In regions c and d, the water-to-ethanol molar ratio is smaller than 5. This number means that any ethanol molecule is almost always in contact with at least one ethanol molecule stochastically. Under this condition, the following association-dissociation equilibrium should be considered as an important process among various association equilibria in the solution.

$$(C_2H_5OH)_{m-1} + C_2H_5OH \overset{K_{m,0}}{\rightleftharpoons} (C_2H_5OH)_m \qquad (5)$$

This type of equilibria was first considered by Kempter and Mecke[32] and modified for the elucidation of the infrared absorption of various alcoholic solutions by Coggeshall and Saier.[33]

As seen from the temperature independence of the spectral patterns, the enthalpy change of this process is much smaller than 1 kcal/mol in region c ($0.18 \leq x \leq 0.5$). This means that the equilibrium constant $K_{m-1}{}^{n+1}$ of the following exchange process is close to unity in the cluster region observed ($4 < m < 9$).

$$(C_2H_5OH)_m + (C_2H_5OH)_n \overset{K_{m-1}{}^{n+1}}{\rightleftharpoons} (C_2H_5OH)_{m-1} + (C_2H_5OH)_{n+1} \qquad (6)$$

Namely, $[(C_2H_5OH)_{m-1}]/[(C_2H_5OH)_m] \approx [(C_2H_5OH)_n]/[(C_2H_5OH)_{n+1}] \approx$ constant. Figure 3 shows that this relation holds approximately for the parent cluster sizes larger than 4 in the solutions with ethanol concentrations of 40-80% ($0.17 \leq x \leq 0.56$). The association equilibrium (reaction 6) with $K_{m-1}{}^{n+1} \approx 1$ is characteristic of the solutions in region c.

In ethanol rich solutions with $x > 0.5$, larger ethanol polymers tend to dissociate with increasing ethanol content and temperature. Long linear chains must be unstable in the solutions with insufficient water molecules where the direct interaction between the ethyl groups (forming hydrophobic bonds) may induce three-dimensional structural change of ethanol clusters.

VI. Conclusion

The isolation of hydrogen-bonding clusters from ethanol-water solutions through adiabatic expansion of mist particles under vacuum revealed the following characteristics of the ethanol-water and ethanol-ethanol clustering in the solutions: (1) The hydrophobic hydration of ethanol is so strong that pure water clusters are not detectable at $x > 0.04$. (2) Ethanol molceules tend to form ethanol polymer chains with surrounding water molecules which make up hydration shells around ethyl groups at the region of $x < 0.04$, but at $x > 0.08$ the hydrogen bonding between water molecules becomes very weak compared with the ethanol-ethanol bond.

Registry No. CH_3OH, 67-56-1.

(31) *International Critical Tables, National Research Council*; McGraw-Hill: New York and London, 1929; p 22.
(32) Kempter, H.; Mecke, R. *Z. Phys. Chem.* **1941**, *16*, 220.
(33) Coggeshall, N. D.; Saier, E. L. *J. Am. Chem. Soc.* **1951**, *73*, 5414.

Carbonaceous Solids as a Model for Adsorption by Dispersion Forces

Edward M. Arnett,* Brenda J. Hutchinson, and Marguerite H. Healy

Contribution from the Department of Chemistry, Duke University, Durham, North Carolina 27706. *Received November 6, 1987*

Abstract: Heats of adsorption of many liquids of widely varying structure are reported on several carbonaceous solids: graphite, anthracite coal, Ambersorb XE-348, and two graphitized carbon blacks, Carbopack B and F. Heats of adsorption on the two graphitized carbon black samples correlate closely with the polarizabilities of the adsorbate and the number of main group atoms in the molecules as might be expected for dispersion force interactions; there is no relationship to the basicities of the adsorbates. Except for the two graphitized carbon black samples, Carbopack B and F, correlation between the various types of carbonaceous solids is poor.

Acid-base chemistry has been used successfully as a means for reducing the complexities of chemical behavior for millions of compounds to a manageable number of parameters. All organic compounds are acids, bases, or both, and most of them can be activated through interactions with other acids or bases. In recent years classical acid-base scales in water at 25 °C[1-3] have been extended to a variety of other solvents and, most significantly, to the gas phase.[4-10] By comparing acid-base properties in these different media there has been considerable success in separating acid-base properties that are inherent to the molecular structures of the isolated acid and base molecules from those properties that are induced by interaction with surrounding solvent.

Many, if not most, reactions of biological and industrial importance occur at liquid-liquid interfaces (micelles, vesicles, etc.)

(1) Bell, R. P. *The Proton in Chemistry*, 2nd ed.; Cornell University Press: Ithaca, 1973.
(2) Kortum, G.; Vogel, W.; Andrusson, K. *Dissociation Constants of Organic Acids in Aqueous Solution*; Butterworths: London, 1961.
(3) (a) Perrin, D. D. *Dissociation Constants of Organic Bases in Aqueous Solution*; Butterworths: London, 1965. (b) Perrin, D. D. *Dissociation Constants of Organic Bases in Aqueous Solution, Supplement*; Pergamon Press: New York, 1982.
(4) Davis, M. M. In *The Chemistry of Non-Aqueous Solvents*; Lagowski, J. J., Ed.; Academic: New York, 1970; Vol. 3.
(5) Arnett, E. M.; Scorrano, G. *Adv. Phys. Org. Chem.* **1976**, *13*, 84.
(6) (a) Taft, R. W. *Prog. Phys. Org. Chem.* **1982**, *14*, 1. (b) Taft, R. W. *Kinetics of Ion-Molecule Reactions*; Ausloos, P., Ed.; New York, 1979. (c) Taft, R. W. *Proton Transfer Reactions*; Caldin, E., Gold, V., Eds.; Chapman and Hall: London, 1975.
(7) Bower, M. T. *Gas Phase Ion Chemistry*; Academic Press: New York, 1979; Vol. 2.
(8) "Evaluated Gas Phase Basicities and Proton Affinities of Molecules; Heats of Formation of Protonated Molecules": Lias, S. G.; Liebman, J. F.; Levin, R. D. *J. Phys. Chem. Ref. Data* **1984**.
(9) Arnett, E. M. *Acc. Chem. Res.* **1973**, *6*, 404.
(10) Arnett, E. M. *J. Chem. Educ.* **1985**, *62*, 385.

0002-7863/88/1510-5255$01.50/0